Report on case studies

Demonstrating the errors related to each manufacturing step from medical imaging to patient application

Deliverable D8

Lead author: VTT

Project 15HLT09 “MetAMMI Metrology for additively manufactured medical implants”.

Due date: 31st May 2019

Submission date: 3rd June 2019

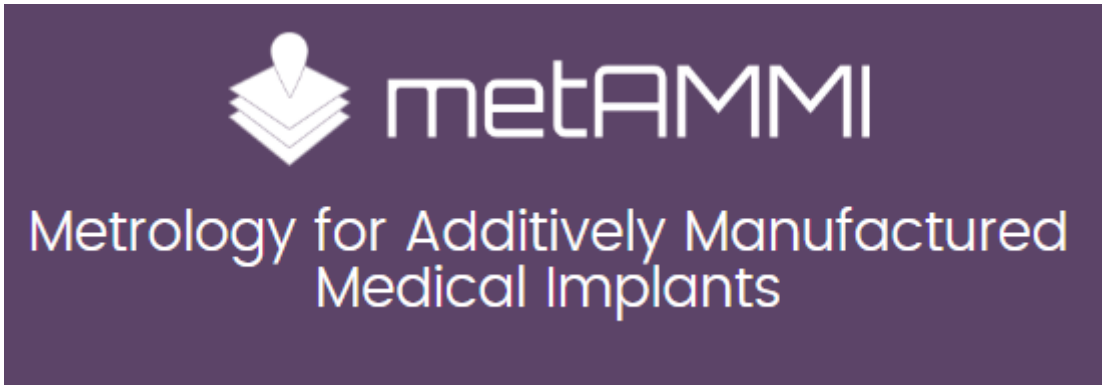

Contents

Introduction

The aim of the case studies is to show up and to quantify the errors related to the different steps within an implantation workflow, from imaging at the very beginning to the final clinical delivery. Thus, users raise awareness on critical steps and can try to avoid pitfalls and try to reduce uncertainties of relevant order of magnitude. Typical steps in body part replication are:

1. Medical imaging

2. Segmentation of relevant tissues for 3D model reconstruction

3. Selection of implant/guide material, type and structure

4. 3D modelling for implant/guide and preoperative model

5. Additive manufacturing and finishing of printed parts

6. Clinical use

Different clinical applications of clinical importance have been selected to study the afore mentioned implantation chain. In some cases only a combination of different steps is accessible. In these cases the combined uncertainty budget of these steps is considered. In all cases the implant or guide efficiency will be evaluated:

- Case 1: Maxillo-facial implant (VTT, Aalto)

- Case 2: Dental guide (SKBS, PAS, PTB, BEGO)

- Case 3: Spinal implant (UNOTT)

- Case 4: Cranial implant (SKBS, PTB)

This document is the deliverable D8 in the Project 15HLT09 “MetAMMI Metrology for additively manufactured medical implants”. This project has received funding from the EMPIR programme co-financed by the Participating States and from the European Union’s Horizon 2020 research and innovation programme.

Case 1: Maxillo-facial implant (VTT, Aalto)

In maxillo-facial surgical procedures, an emerging practise has adopted preoperative virtual planning. The practise initiates with patients diagnosed with maxillo-facial deformity generally caused by injuries, infections, or tumours. The innovative practise involves a process chain, outlined in Figure 1, comprising medical imaging of maxillo-facial region of the patient, segmentation of the medical images, 3D modelling of the patient specific implant, additive manufacturing of the implant and finally, the surgical procedure in which the implant is inserted into the patient. The aim of this case study is to evaluate error propagation of a maxillo-facial end-use implant considering the whole process chain. The study was conducted following the principles of guide to expression of uncertainty in measurement, known as GUM. In compliance with the ethical procedure described in the EU Directive 2010/63/EU, a domestic pig-head depicting a maxillo-facial deformity was made the test subject of this case study as shown in Figure 2.

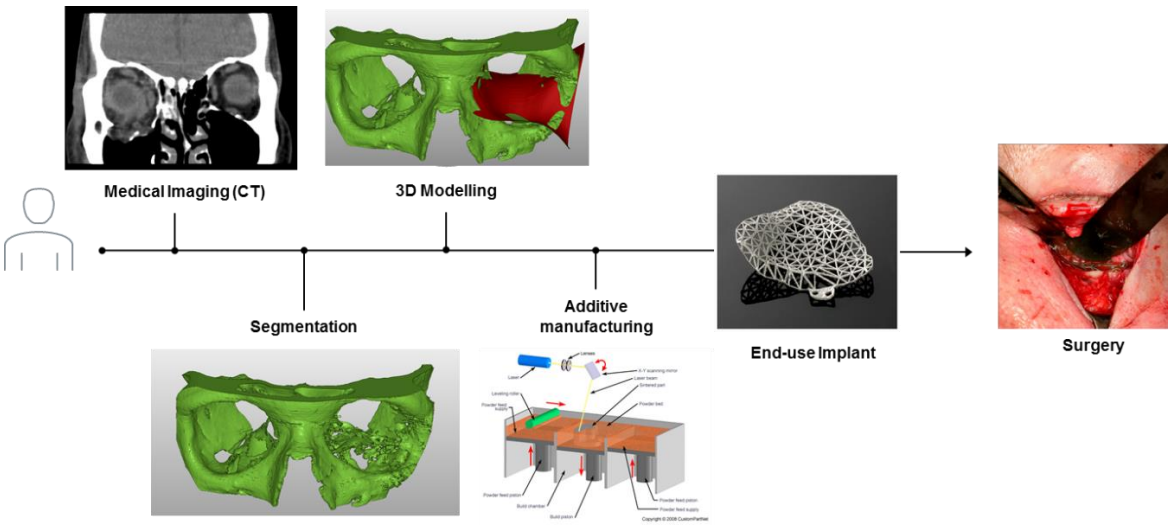

Figure 1. Process chain of preoperative virtual planning of maxillo-facial surgical procedure.

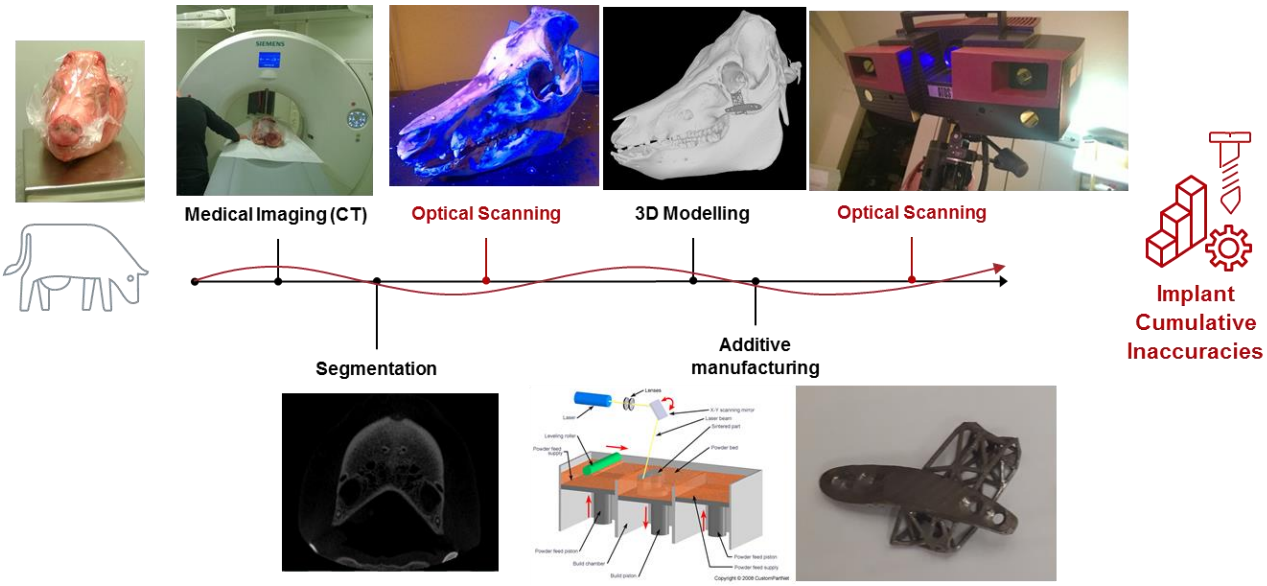

Figure 2. The process of evaluating error propagation of the case study.

Further, a traceable Phantom was developed at VTT Technical Research Centre of Finland Ltd for evaluating the errors associated with medical imaging. The material of the phantom was Polyoxymethylene (POM). This material has a behaviour in medical imaging which is close to bone in terms of linear attenuation coefficient and density. A drawback with this material is sensitivity to humidity uptake. Immediately after the material is primarily manufactured, it expands slightly when absorbing humidity. Nevertheless, it is a stable engineering polymer containing better water resistance than most conventional polymers such as nylon. The process of evaluating medical imaging associated errors is shown in Figure 3.

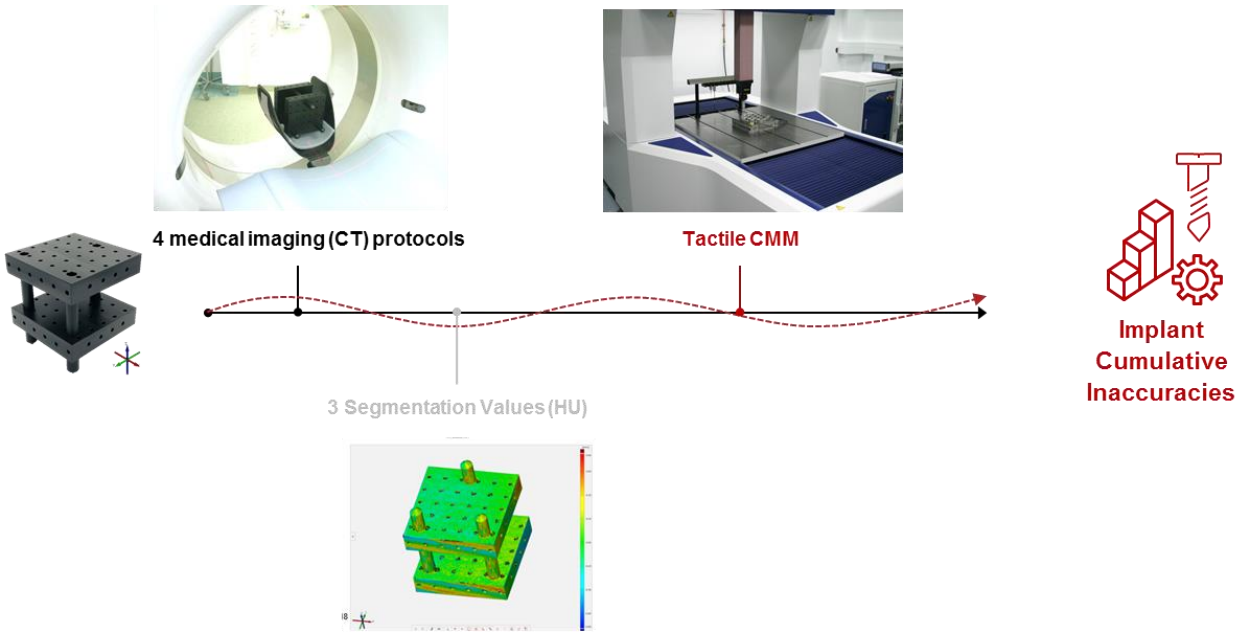

Figure 3. The process of evaluating medical imaging related errors.

The phantom consist of two prismatic blocks and three rods. As seen in the blocks have holes. In addition to hole positions, flatness of surfaces and angles, & distances between surfaces are measurands.

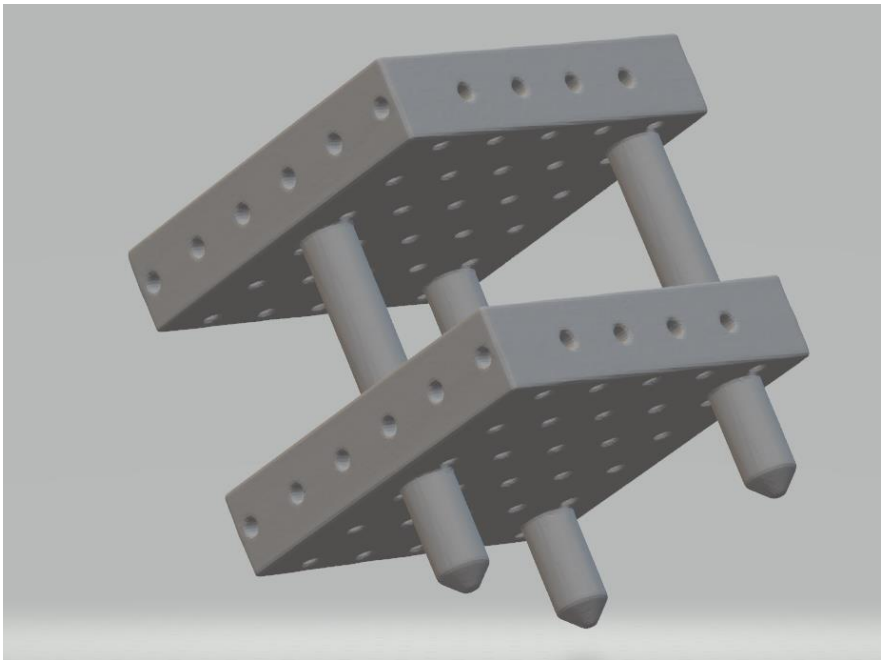

Figure 4. The Phantom

The reference measurements were made with a coordinate measuring machine (CMM), Mitutoyo Legex 9106 at VTT (Figure 5). The CMM is periodically verified with the interferometrically calibrated gauge blocks ensuring a maximum permissible error, $E_{0,\,MPE}$ value, of (0.35 + L/1000 µm), where L is length in mm. The CMM is in a laboratory with a temperature stability of 20°C ± 0.2°C.

Figure 5. The CMM, Mitutoyo Legex 9106, at VTT Technical Research Centre of Finland Ltd.

Using the CMM, 9 planes and 70 holes were measured (Figure 6). These results serve as reference values.

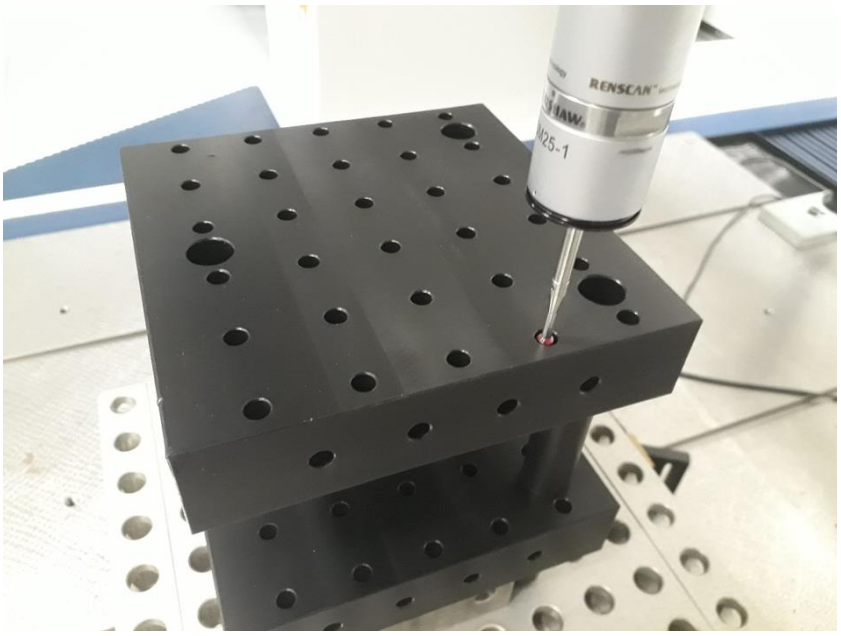

Figure 6. Reference measurements using tactile probe.

In order to evaluate medical imaging process related potential errors, the phantom was scanned at Hospital District of Helsinki and Uusimaa (HUS) using a multi-detector computed tomography (MDCT) system as shown in Figure 7.

Figure 7. Scanning of Phantom at Hospital District of Helsinki and Uusimaa (HUS).

Using GOM Inspect software (made by german company GOM GmbH), hole distances and other measurands were extracted from the STL file generated from the segmented medical computed tomography (CT) scans (Figure 8). For selected medical imaging protocols, hole to hole distances were compared to reference values measured with the CMM. This methodology minimized the effects associated with segmentation of DICOM (Digital Imaging and Communications in Medicine) to STL conversion process and enabled evaluation of errors solely associated with medical imaging. Hence, the volumetric errors of medical imaging were evaluated based on these results. As a result, the linearity ranged at a scale of few microns to hundreds of microns whereas the orthogonality ranged from tens to hundreds of milli-degrees. By assuming a worst case scenario, the volumetric errors for the maximum length of the implant were found to be below 0.1 mm considering all 4 medical imaging protocols.

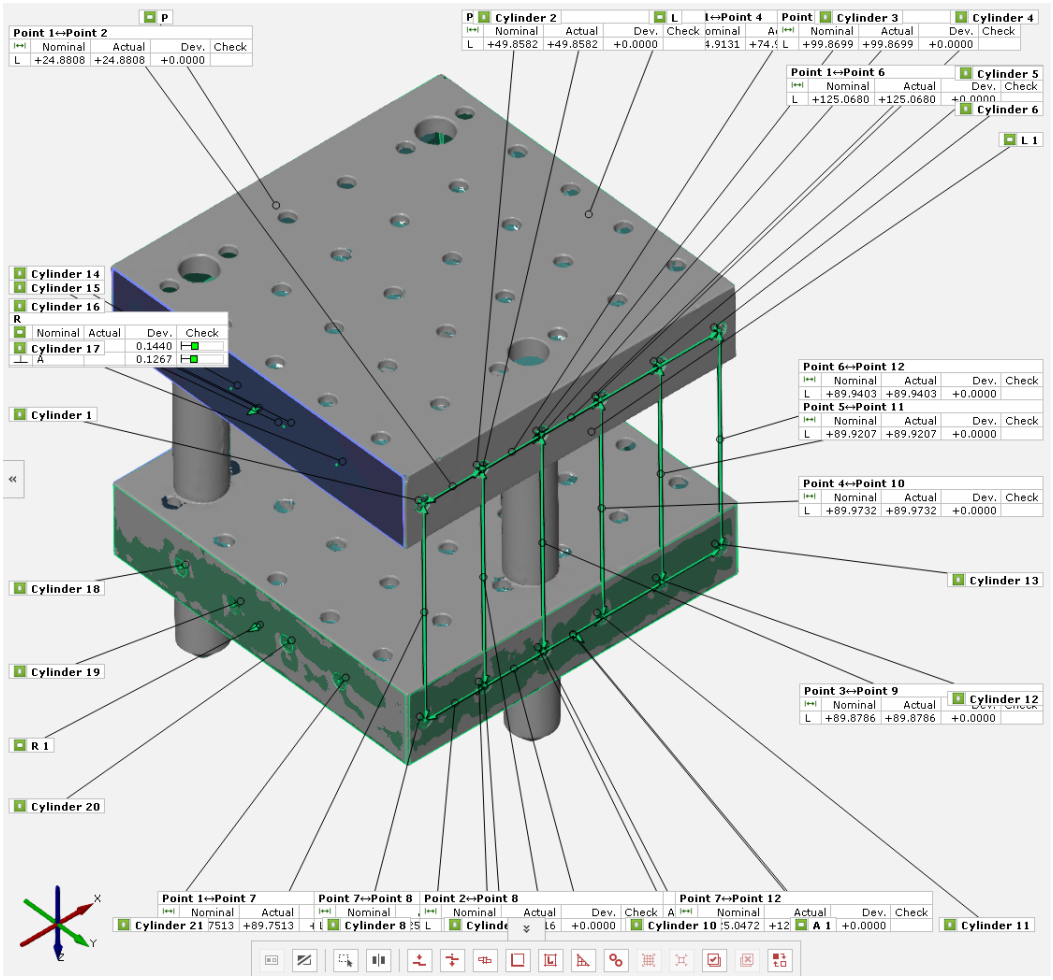

Figure 8. Measurements conducted using GOM Inspect software.

For the evaluation of probable errors associated with segmentation process, the pig-head was also scanned at HUS (Figure 9). The soft tissue was then removed using beetles and the head was also scanned with a fringe projection instrument (Figure 10). In order to estimate the segmented errors, the skull models generated using a combination of 4 different medical imaging protocols and 3 segmentation values were compared with the optically scanned, true surface of the skull. As a result, the segmentation, representative of DICOM to STL conversion, seemed to be associated with quite large errors with a maximum error of 0.7 mm. The results showed significant variation in two different CT reconstructions. Where Type A (J70H) reconstruction kernel generated blocky, coarse surfaces with loss of data (voids), sharp edges, increased artefacts and staircase effect, the Type B (J30S) reconstruction kernel produced smooth surfaces with more data (lower amount of voids) and less artefacts. J30S kernel had higher resistance to the partial volume effect. Although negligible (about 1%), lower CT image thickness of 0.5 mm captured more data than higher CT image thickness of 1 mm.

Figure 9. Scanning of pig-head with medical imaging at HUS.

Figure 10. Scanning of pig-head with fringe projection (optical scanner) instrument.

During the 3D modelling process, a zygomatic bone resection implant was designed using the projections and surfaces of the optimal segmented pig-head skull model (Figure 11). The errors associated with this process arise from the numerical resolution of 3D modelling software which amount to 50 nanometres.

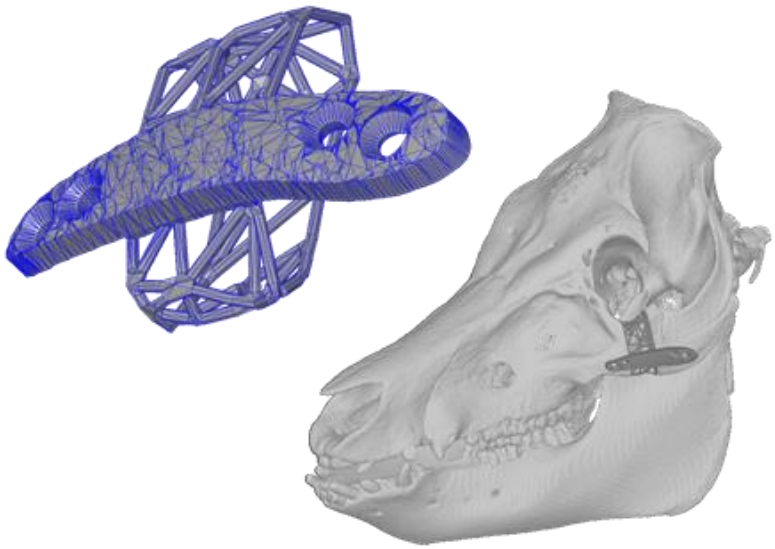

Figure 11. The designed zygomatic bone resection implant on the pig-head skull surface.

Throughout the additive manufacturing process, the implant was additively manufactured in titanium using a laser-based powder bed fusion method (Figure 12). A conventional operator removed the support structures of the implant manually. In order to estimate the manufacturing errors, the resultant implant was optically scanned with a fringe projection instrument and was compared with the nominal CAD model, which revealed errors of about 0.9 mm for the worst-case scenario.

Figure 12. The titanium implants with support structures (top) and without support structures (bottom) additively manufactured .

Finally, the combined and collective error of the implant depicting the worst-case scenario can be fairly significant in maxillo-facial surgical procedures including all steps from medical imaging of the patient to the final implant. The error increases at each step of the process though 3D modelling error is quite insignificant. The total cumulative error amounts to 1.6 mm for the ready implant (Figure 13). This is calculated for one boundary condition. If we consider a case that involves two segmented boundary surfaces, then the segmented error is increased by two times. This yields a cumulative error of 2.2 mm, which can be quite significant. Since uncertainties of the reference measurements were significantly smaller than the manufacturing process uncertainty, they were neglected from the calculations.

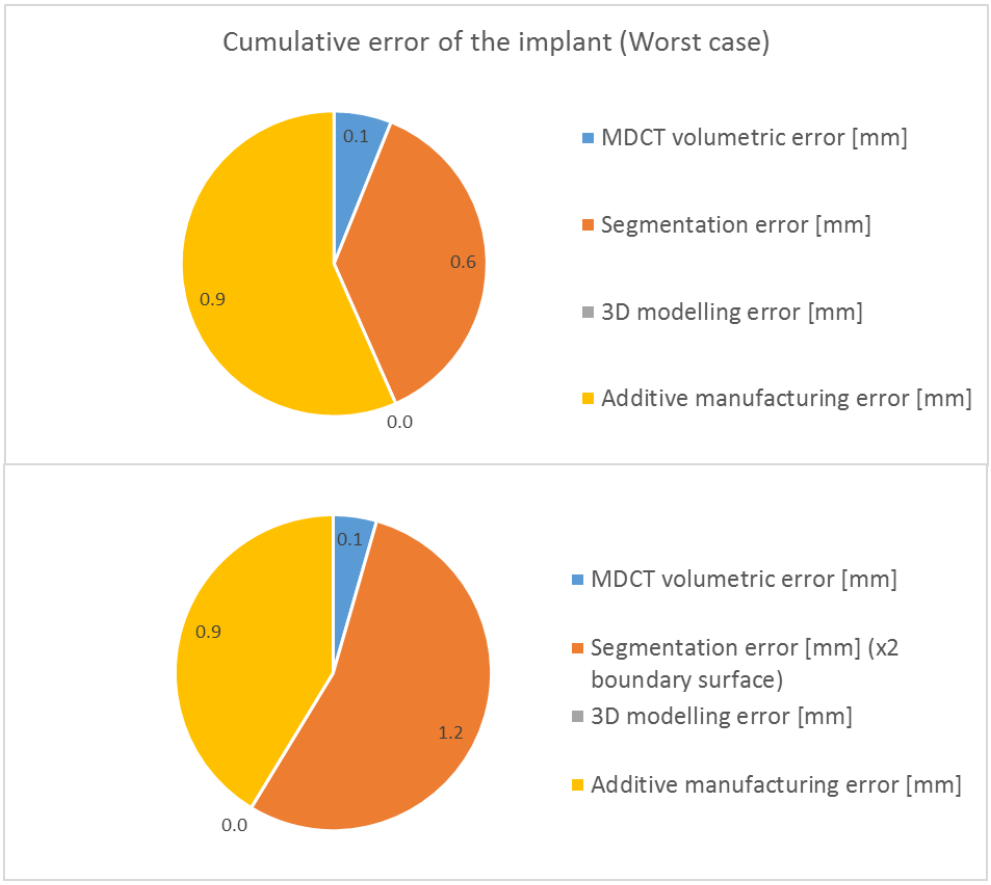

Figure 13. Cumulative error of the implant with one boundary surface (Top) and with two boundary surfaces (bottom) [results to be submitted in a scientific journal].

In conclusion, the cumulative inaccuracies estimated in this case, aid practitioners in developing and verifying suitable medical practises.

Case 2: Dental guide (SKBS, PAS, PTB, BEGO)

Dental guides are mass market products. Although, AM guided implantations become more and more popular, there is a lack of systematic knowledge on different factors influencing the overall uncertainty of this process as well as the clinical consequences resulting from these uncertainties. Thus, the main objective of our clinical case study related to dental guides was the characterization and quantification of possible uncertainties and tolerances while planning and additively manufacturing dental drilling guides. An example of such a product as well as its fabrication process is shown in Figure 14.

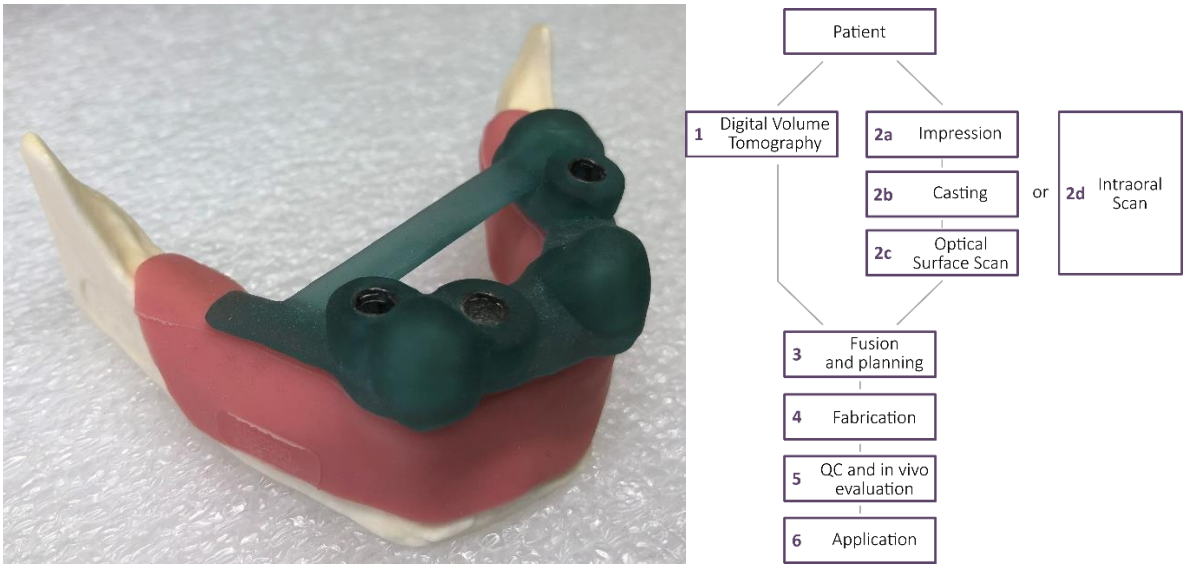

Figure 14: Left: Additively manufactured dental drilling guide from BEGO mounted onto a dental training model. Right: Process to create an additively manufactured and patient individual surgical drilling guide for dental implantation.

The complete production chain for a dental drilling guide generally consists of the following steps:

1. Acquisition of a dental digital volume tomogram (DVT) or a computed tomography (CT). This becomes necessary, as bony structures as well as nerve channels cannot be visualized with other techniques. 3D X-ray image data with resolution on the micrometre scale enables surgeons to plan implant positions with sufficient safety distance from delicate structures (such as nerves or dental roots) and with optimal esthetical results.
2. Acquisition of a high trueness surface profile of the remaining denture using either conventional impression techniques and subsequent optical surface scans (a – c) or more convenient intra oral scanners (d). Acquisition of the surface profile is necessary as the guide has to be mounted on the remaining denture and thus, a good as possible fitting on denture and oral mucosal membrane is essential.
3. The results from step one and two (3D x-ray and optical surface data) are imported into a CAD software dedicated for planning dental implantations. The datasets are (semi-)manually aligned onto each other with respect to the surface of the teeth. The implants are virtually

planned and drilling holes are defined with the desired position and angulation of the implant in mind. Based on the plan, the design of drilling guide is computed.

4. Using additive manufacturing such as steorelithographic 3D printing, the polymer part of the guide is produced. Metal sleeves to guide the drill are inserted manually, afterwards.
5. After finishing the product quality control procedure, the guide is inserted into the oral cavity and its fitting is checked by the surgeon.
6. Finally, holes to fit the implants are drilled manually under guidance of the AM product.

SKBS, PAS, PTB and BEGO analysed thoroughly the influence of every step within the planning, production and application chain on the uncertainty budget:

Step 1: Dental Volume Tomography

Image quality of two representative DVT systems was considered quantitatively by analysing image distortion, resolution, and trueness of CT numbers with technical phantoms.

Image distortion was addressed using a traceably calibrated multisphere distance normal. All possible distances between the spheres were analysed accordingly. We observed average distance deviations up to 250 µm, depending on the z-position (up to 0.7 % relative to the corresponding reference distance values).

The modulation transfer function (MTF) was used as measurand of the axial resolution. MTF was determined for different positions within the field of view in all directions using a sphere phantom. For the inspected systems, the MTF (10%) varied between 4 and 10.6 lp/cm usually with a drop in resolution for more remote positions.

Generally, DVT systems do not provide CT-numbers in a quantity “Hounsfiled units” (HU) like conventional CT systems. Anyhow, a well-defined relation between electron densities and signal values is essential for surface extraction, even for DVT systems used in implantology. Thus, the trueness of signal values was evaluated for relevant high contrast materials as well as air and water. For the system under inspection, deviations up to 100% relative to the calculated reference CT-numbers were observed. Furthermore we found, that the measured CT number of the solid water® base material varied between 120 HU and 190 HU within scans of the different material inserts.

In a second approach, a retrospective analysis based on 10 representative clinical cases, showing different dental status, was conducted. For this, PAS selected cases with available optical surface scan of a gypsum model and DVT. SKBS created STL data from those DVT sets with different surface reconstruction parameters. The STLs from the DVT files were compared to the corresponding optical surface scans. Deviations were determined. The influence of jaw status and DVT-parameters on the overall uncertainty were assessed.

Limited visual image quality, e.g. due to heavy beam hardening artefacts, might influence the quality of the fusion of DVT and STL-files. This study was conducted based on five representative cases with acceptable and poor image quality. For each case, the manual processes of data fusion and planning of the drilling guides was repeated threefold. Deviations between the three resulting STL files for each case were assessed, afterwards, by comparing their surfaces and by calculating

the geometric deviation of drilling holes that would result from usage of those guides. Surprisingly, no clear dependence of the precision of fusion process on the visual image quality could be observed.

Clinically relevant conclusions based on our findings and our general experience were included in the good practice guide on planning and additively fabricating dental drilling guides.

Step 2a: Trueness and precision of moulding materials

The influence of different moulding materials on the process was assessed. Studies were performed on an artificial dental reference model. Within this study branch the surface of the reference object was compared to the surface of gypsum casts that resulted from the use of different moulding materials as well as moulding trays. The geometry of the reference object as well as the study objects were determined prior to the studies with an industrial XCT at PTB.

The following research tasks were conducted:

- Geometrical distortion, based on a study from three representative moulding materials.
- Geometrical distortion that results from the moulding tray. In this task, results from a process using a conventional tray and from a process using individualized trays were compared.

The resulting surface to surface distances between reference and result was typically smaller than 400 µm for alginate and smaller than 200 µm for polyether as well as silicone moulding material. No relevant difference was observed for the use of individually made and conventional metal trays.

Step 2b: Trueness and precision of gypsum products

Using the same reference model as being used in step 2a, the trueness of three representative gypsum products was considered. Again, geometrical deviation between the reference object and den gypsum casts were assessed. As in step 2b, the surfaces were determined on basis of XCT scans conducted by PTB.

Surface to surface distances between reference and the resulting models were smaller than approximately 200 µm for all gypsum types under consideration.

Step 2c: Desktop optical surface scans

Using the dental model and a gypsum cast of a real patient, trueness, precision and user variability of multiple different desktop optical surface scanners were assessed in relation to a reference XCT scan of the model and gypsum cast conducted at PTB.

Surface to surface distances between reference CT and optical scans were found to be below 60 µm. No relevant user to user variation was observed. Precision for each scanner was better than 20 µm.

Step 2d: Intraoral scanning

Intraoral scanning may serve as alternative to steps 2a to 2c and is more and more employed in the clinical practice. We considered trueness of one intraoral scanning system in vitro and precision in vivo since high precision reference XCT data cannot be obtained in humans for ethical reasons. Several scanning conditions were considered. In vitro trueness was better than 100 µm. Intraoral precision was better than 150 µm in two different patients.

Step 3: Fusion and planning

Variation of the manual fusion and planning results was observed on basis of data from a real patient and a dental in vitro model. BEGO fused DVT and STL datasets of both cases threefold from scratch. Based on those fusions, drilling guides were designed, always assuming identical implantation demands. 4 drilling holes were designed for each planned case at different positions and with different angulations.

The average deviation of the angle of the drilling holes was in the range of 0.25° and 0.45°. The average translation of the drilling holes between different realisations of the same planning task was in the range of 180 µm and 260 µm assuming a drilling depth of 20 mm. Surface to surface distances were smaller than 50 µm for the in vitro model and 80 µm for the human model and were mostly introduced by small deviations of the planned guiding sleeves and not the general surface.

Step 4: Fabrication

BEGO additively manufactured five guides from one single realization of step 3. Five drilling guides were milled by a third company based on the same CAD file for comparison. PTB performed XCT imaging on all items, first after the fabrication of the plastic part and second after the insertion of the metal sleeves. All scans were compared for trueness and precision, especially concerning deviations in the drilling angles and translations of the drilling holes.

For AM products, average deviation of drilling angles between CAD and the fabricated products was in the order of 1.5°. The average precision over all realizations was 0.7°. The average translation of drilling holes in 20 mm depth was 470 µm compared to the CAD. The precision was 240 µm. For the milled guides, angular trueness was approximately 1.7° and the average translation was found to be 1.7 mm on average in 20 mm depth compared to CAD. The angular precision was 2° and the precision of drilling deviation in 20 mm depth was 0.63 mm on average. However, one needs to consider, that only 3 of 5 holes could be realized due to geometric limitations of the milling device.

Step 5: Quality control and in vivo evaluation

A detailed protocol for quality control was compiled from the findings within the project and clinical experience and included in the good practice guide on planning and additively manufacturing of dental drilling guides.

Step 6: Application

A detailed collection of practical recommendations for application of dental drilling guides was compiled based on clinical experience and included in the previously mentioned good practice guide on planning and additively manufacturing of dental drilling guides.

The detailed analysis of possible planning and manufacturing deviations presented above is highly relevant for characterization and optimization of the individual process steps. However, overall planning and manufacturing uncertainties for individual patients must not be concluded from these numbers due to the patient individual and complex intraoral geometry. The results might be considered as hints on production steps where larger uncertainties are to be expected and might lead to an increased effort to lower these tolerances.

Independent of the inspection of different production steps and their related error components, the overall uncertainty of the complete chain was examined in a second case study. Relevant quantities in the second case study were angular deviations and translation of the resulting drilling holes at the point of clinical use of the drilling guides. This cumulative manufacturing deviation includes all influences from every process step. Since postoperative DVT scans on humans are not possible for ethical reasons, a study was set up using training models for dental implantations. Thus, the study was conducted in vitro and geometrical precision was assessed using metrological XCT scans, acquired by PTB.

Five different planning and application processes were studied, each with a separate model. Models one to three were treated using the same parameters as considered in the previously already mentioned productions steps. Models 4 and 5 were built, following the standard clinical procedures of PAS including additive manufacturing within PAS's laboratory. The processes were based on conventional moulding as well as intraoral scanning.

Within the study, at first, reference holes were drilled to the implantation model and a reference XCT was acquired. The position of the holes reflected the desired implant placement positions and angles and are the reference against which the drilling holes that result from the application of the guides were compared. Afterwards the holes were refilled. The aim of the subsequent manufacturing process steps was to fabricate guides that allow a redrilling of the planned holes as exactly as possible. The drilling holes at the end of the production and application chain were determined on basis of XCT scans from PTB and deviations were analysed.

Angular deviations between the reference holes and finally drilled holes were up to 5°. Resulting translation of the drilling holes at maximum depth was below 1.8 mm.

Case 3: Spinal implant (UNOTT)

Pedicle Screw Drill Guide

Pedicle screws are the primary technology for providing mechanical attachment to the spine. They are used in all aspects of spine surgery including deformity correction, trauma, cancer surgery and treatment of degenerative disease. The global market is currently worth $4 billion with 6 million screws implanted annually. The market is growing and global with primary territories being the USA and Canada, Europe, Japan and Australia. Emerging markets in China and India will further increase market growth.

Pedicle screws have significant drawbacks; they are time consuming to place (incurring significant radiation doses for both patient and surgeon) and have major safety issues – primarily misplacement. A typical deformity correction might use 24 screws each taking 15 minutes to insert. There is a 3-30% chance each screw will be misplaced with the screw fracturing the pedicle and entering space occupied either by spinal cord or segmental nerves. There is therefore a significant risk of paraplegia.

Drill guides, custom manufactured by additive manufacture, are therefore entering the market with the aim of reducing surgery times and improving patient outcomes. This study presents an evaluation of imaging and post processing on the precision of drill guide design.

A human lumbar spine (including discs and ligaments) was imaged using the normal clinical protocols on an imager (in standard clinical use) at the Nottingham University Hospitals (NHS) Trust Queen's Medical Centre (Figure 15). The imager was a Phillips Ingenuity Core 128 imager using the 5B/C Thoracic and Lumbar Spine helical scan protocol. This has an in-plane voxel size of 0.734 mm and a slice thickness of 0.5 mm.

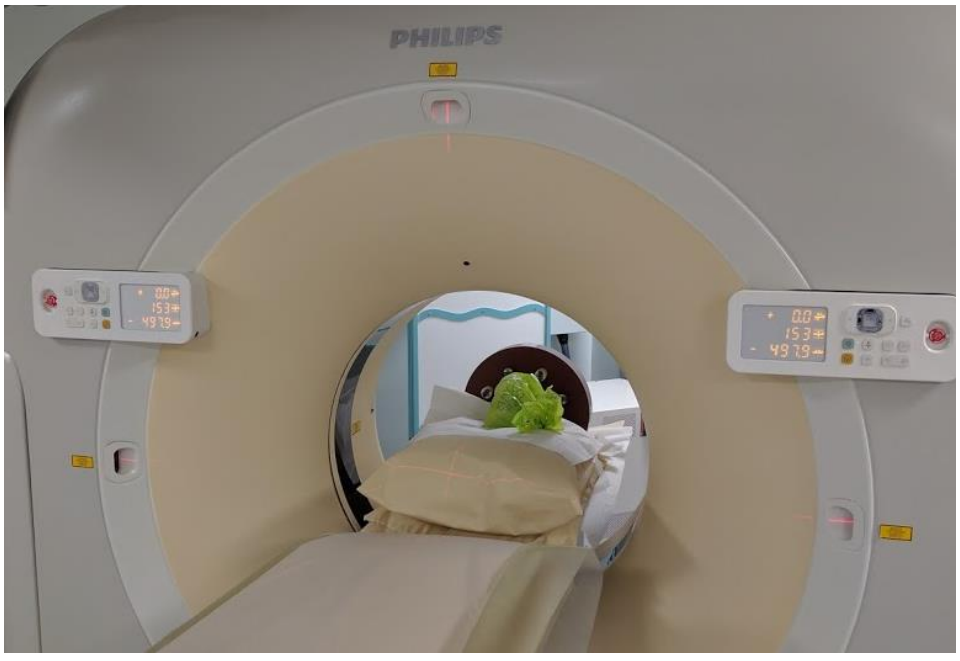

Figure 15: Spinal segment during image acquisition within the Phillips CT clinical imager

This image dataset was used as the gold standard for the geometry of the spinal segment and was segmented using standard ISO 50% protocols (with a threshold of 114 Housfield units) to give a solid model of the spine (Figure 16).

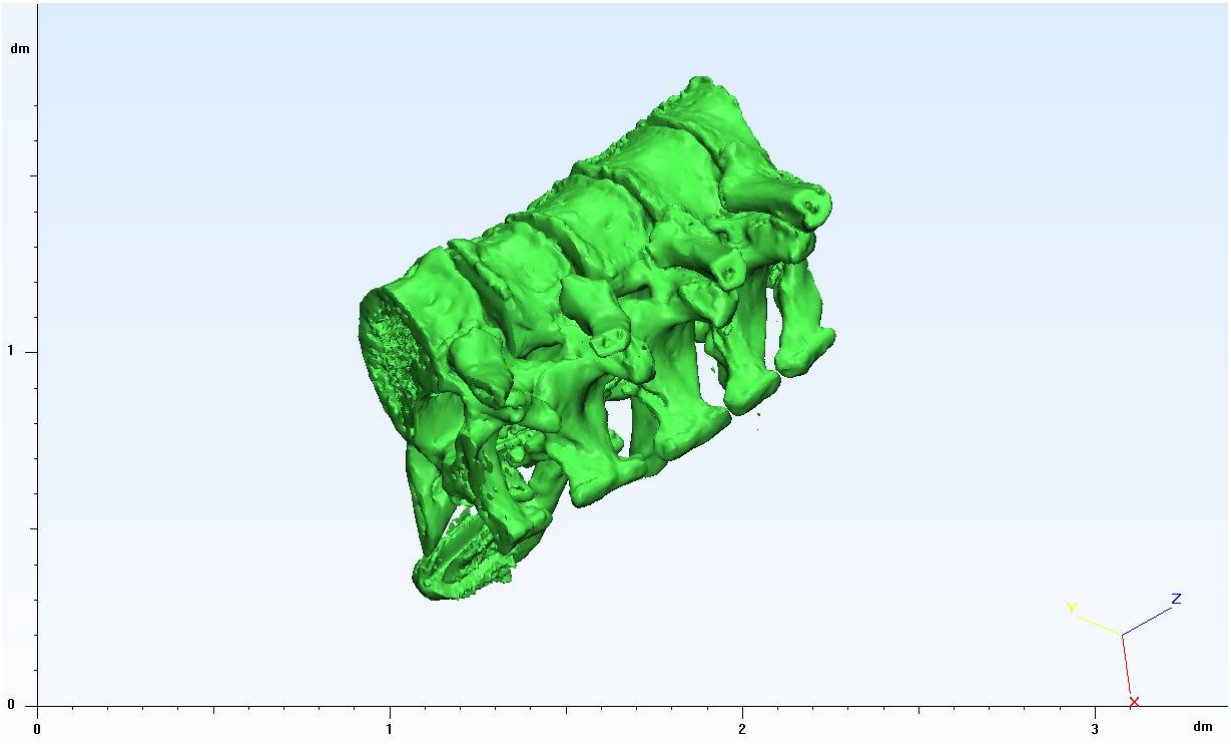

Figure 16: Solid model of the spine with voxel size 0.734x0.734x0.500 mm

Different imaging parameters and post processing methods were simulated by resampling this gold standard dataset to degrade the spatial resolution and provide surface smoothing as in Table 1.

Spine models	**Voxel size**	**Binning method**	**Post-processing**
Full resolution	0.734 mm × 0.734 mm × 0.5 mm	No binning	None
High	1.468 mm × 1.468 mm × 0.5 mm	2× in X&Y	None
Medium	2.202 mm × 2.202 mm × 1 mm	3× in X&Y, 2× in Z	None
Low	4.404 mm × 4.404 mm × 1 mm	6× in X&Y, 2× in Z	None
Smooth	0.734 mm × 0.734 mm × 0.5 mm	No binning	Smoothing • 3 iterations • smooth factor = 0.4 • compensate for shrinkage

Table 1: parameters used to simulated different imaging and post processing parameters

The placement of standard 4 mm diameter, 35 mm long pedicle screws were planned as in normal clinical practice (Figure 17a). Drill guides, based on a current commercial design, were then designed, based on each of the geometrical models (Figure 17b). Finally, each of the drill guides was fitted (virtually with a 3 point contact and overlap depth of < 20 µm) 10 times onto the full resolution spine model. Analysis of deviation of screw orientation and tip position was then performed compared to the planned orientation (Figure 17c).

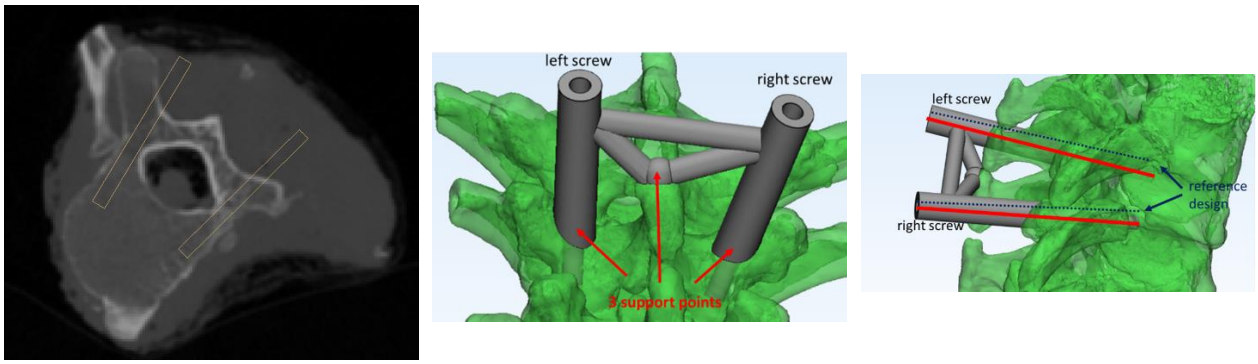

(a) (b) (c)

Figure 17: (a) planning screw placement, (b) drill guide design, (c) analysis of screw placement

Screw placement was found to be consistently within 0.5° of planned orientation and 1 mm tip position for spatial resolutions up to 1.468x1.468x0.5 mm with no smoothing (Figure 18). Smoothing, even at highest resolution was found to greatly increase the variability of screw placement (Figure 18).

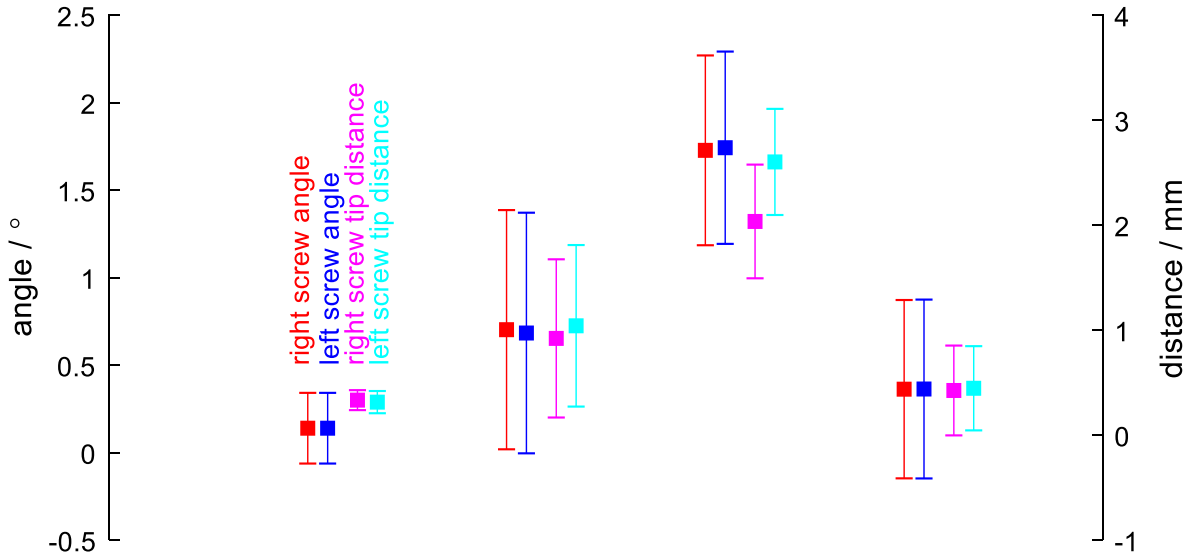

Figure 18: Precision of screw placement

In 11 cases, 10 for the lowest resolution and 1 for the smoothed models, the screw was found to have breached the cortical bone of the pedicle (Figure 19). Such breaching would be a significant clinical complication.

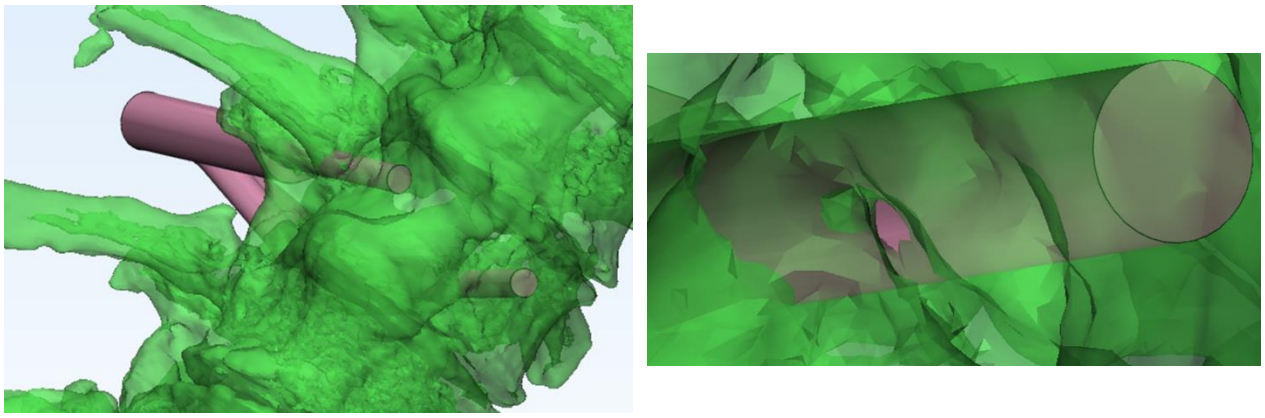

Figure 19: example of screw breaching cortical bone

This study therefore makes the following recommendations:

- Clinical datasets with voxel size > 2.2x2.2x1 mm are not used for pedicle screw guide design.
- Ideally clinical datasets with voxel size < 1.5x1.5x0.5 mm are used for pedicle screw guide design.
- Surface smoothing post processing is not used for pedicle screw guide design.

Custom intervertebral body fusion cage

Current standard clinical practice for spinal fusion is to use intervertebral body cages. These have a variety of different designs according to surgical approach (anterial, posterior, transforaminal). Cages typically come in a range of sizes but are not customised for endplate geometry. However, additive manufacturing techniques are increasingly being used for manufacture of such cages due to the ease of production of appropriate porous/trabecular structures and surface textures. There is also good evidence that a congruent fit between the cage and the adjacent vertebral bodies reduces focal loading (and therefore pain) and improves bone ingrowth and secondary fixation.

The same high resolution and degraded resolution datasets as used for the pedicle screw study above were used. A simplified, solid, cage was designed to fit each model and the fit of each of these cages was analysed relative to the high resolution model. The results are presented in Figure 20.

Voxel Size/Post Processing	Overlap (negative = penetration into bone)
0.734 × 0.734 × 0.5 mm Smoothed	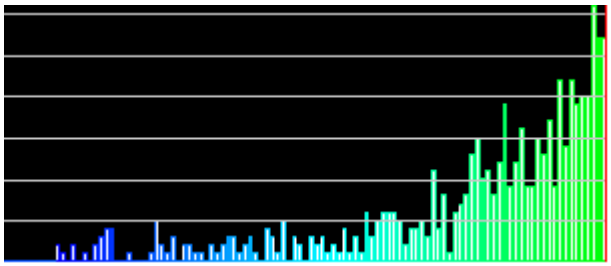 -1.35 mm 0 mm
1.468 × 1.468 × 0.5 mm	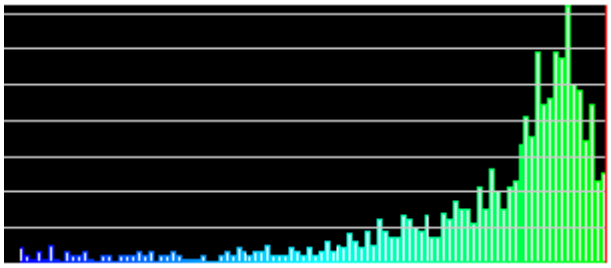 -1.35 mm 0 mm
1.468 × 1.468 × 0.5 mm	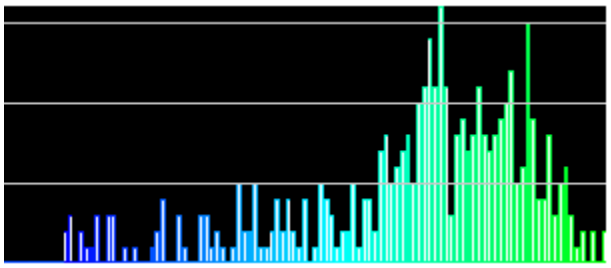 -1.35 mm 0 mm
4.404 × 4.404 × 1.0 mm	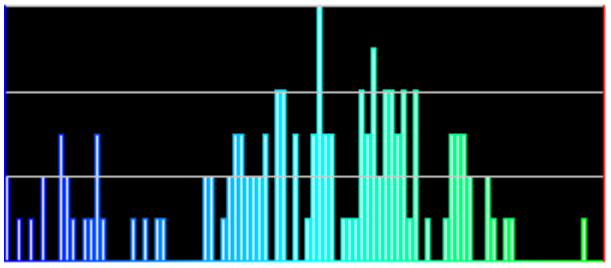 -1.35 mm 0 mm

Figure 20: Sensitivity of cage endplate fit to resolution and smoothing

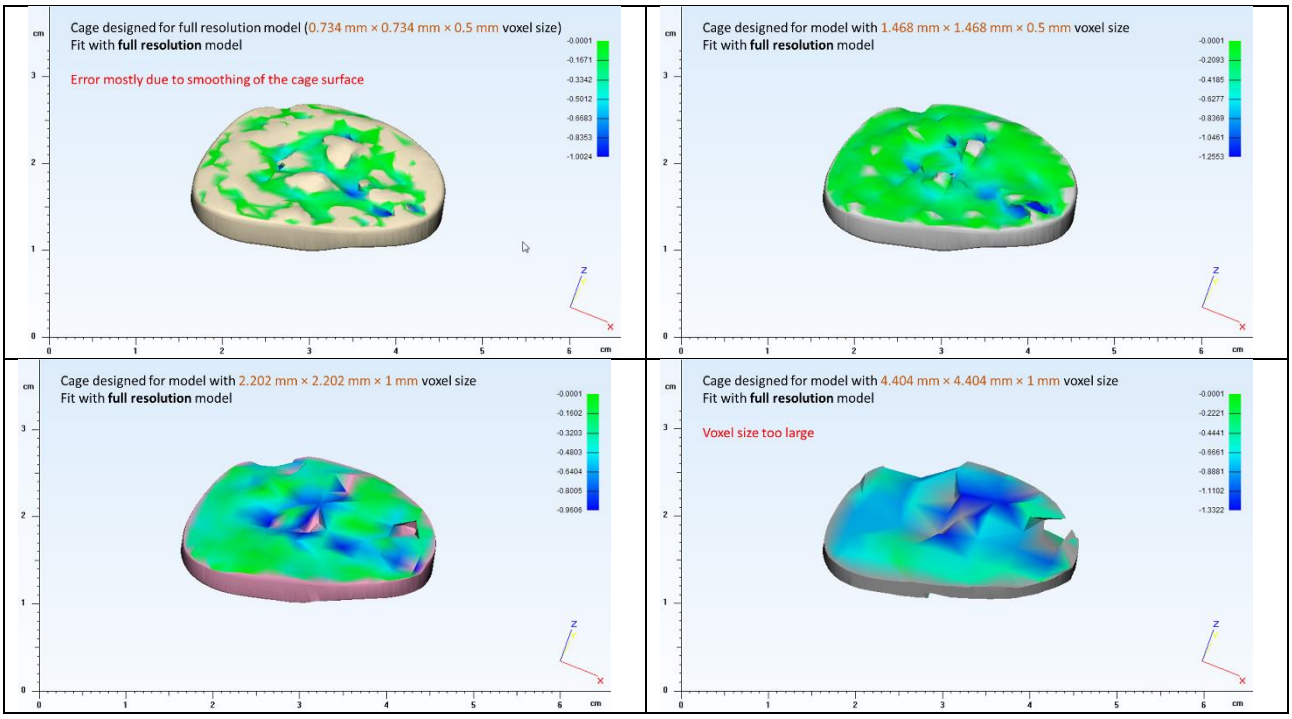

Figure 21: Spatial distribution of fit error with resolution and smoothing

Figure 21 shows the spatial distribution of fit error across the vertebral endplates. It can be seen that smoothing and resolution better that 2.2 x 2.2 x 1.0 mm introduce very few large areas where fit is worse that 0.5 mm.

This study therefore makes the following recommendations:

- Clinical datasets with voxel size > 2.2x2.2x1 mm are not used for design of intervertebral cage endplate design.
- Limited surface smoothing post processing is suitable for design of intervertebral cage endplate design.

Case 4: Cranial implant (SKBS, PTB)

The main goal of this clinical case study was the characterization and quantification of possible uncertainties and tolerances while planning and additively manufacturing implants to treat cranial defects. An example of such a product as well as its fabrication process is shown in **Figure 22**

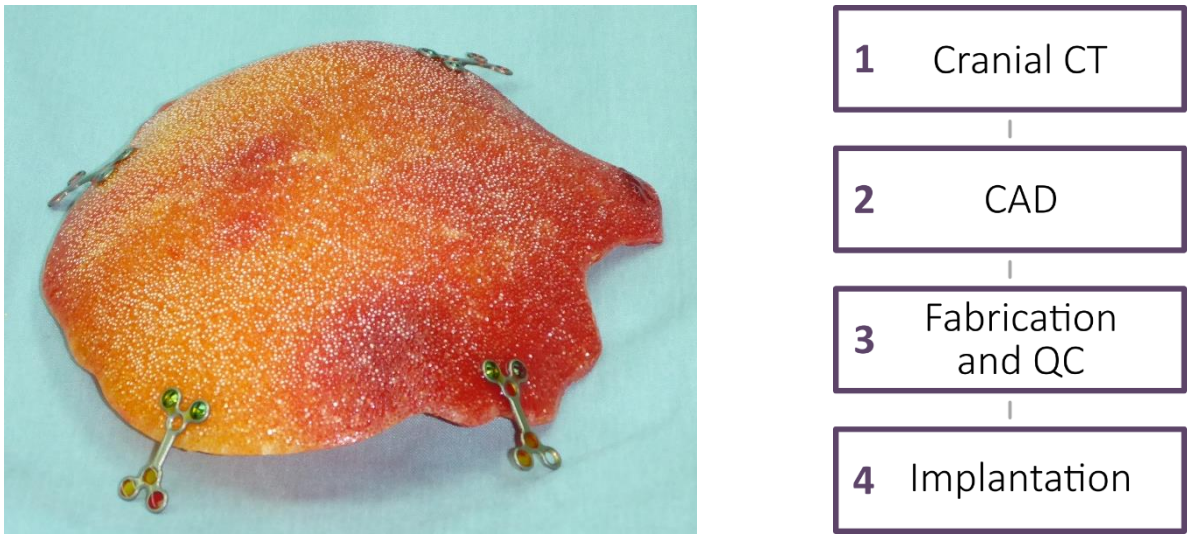

Figure 22: Left: Cranial implant prepared for immediate application. Right: Process for the patient individual additive fabrication of such cranial implants.

The complete production chain for such cranial implants is as follows:

1. Acquisition of a cranial computed tomography according to manufacturer guidelines
2. Computer assisted design of the implant
3. Additive manufacturing of a mould, moulding with the desired material and quality control.
4. Intraoperative optimization and implantation

The fabrication process is solely based on a basic cranial CT. Thus, first studies focused on possible inherent precision degrading influences. Productive clinical CT protocols are highly standardized and optimized and a systematic exploration of the protocol parameter space with patients is thus unethical. Therefore, in addition to the analyses made with technical phantoms in other activities of the MetAMMI-project, studies were conducted to investigate the influence of certain protocol parameters using a phantom, made of a real human skull, which is embedded in resin. The build-up of this skull phantom provides realistic scatter properties.

This skull phantom was thoroughly examined in a medical XCT, which is typically used for acquiring the CT scans for planning cranial implants. An XCT scan of the skull phantom by PTB served as reference dataset. We identified slice thickness and distance as well as the sharpening characteristics of the reconstruction kernel and the acceleration voltage as most influential parameters. Generally, deviations up to 1.7 mm were observed. In the worst case of a reconstruction with 5 mm slice thickness, deviations up to 2.2 mm were measured.

The provider of the cranial implants refused detailed information on the production process. Thus, in several steps, assumptions on reasonable procedures were necessary, such for the surface

extraction algorithm. We estimated a CT number-cutoff approach, which is the easiest and most common practice in medicine. Following this approach, the uncertainty of surface extraction was evaluated. Analysis was done on basis of ten representative conventional cranial CTs from two different machines and reconstructed with different clinical protocols. Since head CTs are well comparable, highly standardized studies, the surface was determined using 6 different, realistic cut-off values, each deviating from the nearest others by 100 HU. The surfaces of all STLs were compared against the reference STL with optimal CT# of a certain case and deviations are expressed in µm/HU. Those uncertainties were smallest, when sharp kernels and thin slices were used. For soft kernels and 5 mm slices, uncertainties up to 2.2 µm / HU were observed.

There was no direct access to in process samples or CADs to analyse the fabrication process stepwise concerning precision and trueness. Anyhow, for clinical reasons, neurosurgeons tend to optimize implants intraoperatively by manual milling for perfect fitting. This becomes necessary as the structure of the bony rim is subject to changes in the time between acquiring the preoperative CT scan and the final implantation. Since the implantation is conducted in sterile conditions, hygiene and time forbid thorough metrological characterization of this step as well. Therefore, the fabrication and implantation process was treated en block and analysis was conducted based on retrospectively available pre- and the post-surgery medical CT data.

15 clinical cases were assigned to the study. Only cases without any remaining bone in the cranial defect zone were included as this limits the clear detectability of the remaining bone rim. 5 cases received pre and post-surgery CT with comparable technical parameters (e.g. same machine and same slice thickness). Datasets have been compared, which, however, was limited because of the use of deviating exposure and reconstruction parameters in the pre- and post-surgery scans. These deviations result from deviating clinical tasks for the studies.

The manufacturing and shipping of the implant takes several weeks. Thus, in several cases the geometry of the bone rim changes in the meantime, due to bone degradation or scar development. The effect was assessed quantitatively. Deviations up tow 1.3 mm were observed.

In most cases, the post implantation CT reveals rather prominent remaining distances between the implant and the bone rim. The average gap size was around 5.8 mm. In some cases, in particular in the temporal region, deviations up to 15 mm were observed. According to the involved neurosurgeons, the size of the gaps does not lead to any problems. This is because the implants are fixed with clips at the bony rim and remaining gaps are filled with scar material within time.

The studies were conducted in close collaboration with SKBS' neurosurgery and radiology department and information about clinical usability factors and general opinions were collected. It turned out, that the clinical acceptable tolerances of the process are far above the uncertainties achievable in the production process. Thus for currents clinical needs, existing uncertainties seem to be it a negligible level for case of cranio-implants.